

# Accepted Manuscript

Pi5 and Pi6, two undescribed peptides from the venom of the scorpion *Pandinus imperator* and their effects on K<sup>+</sup>-channels

T. Olamendi-Portugal, A. Csoti, J.M. Jimenez-Vargas, F. Gomez-Lagunas, G. Panyi, L.D. Possani

PII: S0041-0101(17)30149-6

DOI: [10.1016/j.toxicon.2017.05.011](https://doi.org/10.1016/j.toxicon.2017.05.011)

Reference: TOXCON 5628

To appear in: *Toxicon*

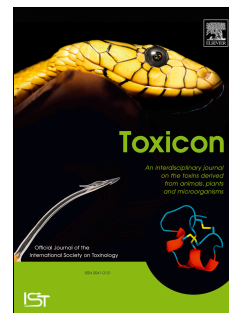
Received Date: 24 March 2017

Revised Date: 6 May 2017

Accepted Date: 9 May 2017

Please cite this article as: Olamendi-Portugal, T., Csoti, A., Jimenez-Vargas, J.M., Gomez-Lagunas, F., Panyi, G., Possani, L.D., Pi5 and Pi6, two undescribed peptides from the venom of the scorpion *Pandinus imperator* and their effects on K<sup>+</sup>-channels, *Toxicon* (2017), doi: 10.1016/j.toxicon.2017.05.011.

This is a PDF file of an unedited manuscript that has been accepted for publication. As a service to our customers we are providing this early version of the manuscript. The manuscript will undergo copyediting, typesetting, and review of the resulting proof before it is published in its final form. Please note that during the production process errors may be discovered which could affect the content, and all legal disclaimers that apply to the journal pertain.



1 **Pi5 and Pi6, two undescribed peptides from the venom of the scorpion *Pandinus imperator***  
2 **and their effects on K<sup>+</sup>-channels**

3

4 Olamendi-Portugal, T.<sup>a,+</sup>, Csoti, A.<sup>b,+</sup>, Jimenez-Vargas, J.M.<sup>a</sup>, Gomez-Lagunas, F.<sup>c</sup>, Panyi, G.<sup>b</sup>,  
5 Possani, L.D.<sup>a,\*</sup>

6

7 <sup>a</sup>Departamento de Medicina Molecular y Bioprocesos, Instituto de Biotecnología, Universidad  
8 Nacional Autonoma de Mexico, Avenida Universidad, 2001 Cuernavaca, Morelos 62210 Mexico

9 <sup>b</sup>Departamento de Fisiología. Facultad de Medicina, Universidad Nacional Autonoma de  
10 Mexico, Ciudad de Mexico 04510, Mexico

11 <sup>c</sup>Department of Biophysics and Cell Biology, Faculty of Medicine, Research Center for  
12 Molecular Medicine, University of Debrecen, 1 Egyetem ter, Debrecen, 4032, Hungary.

13

14 <sup>+</sup>Contributed equally to the work

15

16 \*Corresponding author

17 Lourival D. Possani, E-mail: possani@ibt-unam.mx

18

19

20 **ABSTRACT**

21 This work reports the isolation, chemical and functional characterization of two previously  
22 unknown peptides purified from the venom of the scorpion *Pandinus imperator*, denominated  
23 Pi5 and Pi6. Pi5 is a classical K<sup>+</sup>-channel blocking peptide containing 33 amino acid residues

24 with 4 disulfide bonds. It is the first member of a new subfamily, here defined by the systematic  
25 number  $\alpha$ -KTx 24.1. Pi6 is a peptide of unknown real function, containing only two disulfide  
26 bonds and 28 amino acid residues, but showing sequence similarities to the  $\kappa$ -family of K-  
27 channel toxins. The systematic number assigned is  $\kappa$ -KTx2.9. The function of both peptides was  
28 assayed on *Drosophila Shab* and *Shaker* K<sup>+</sup>-channels, as well as four different subtypes of  
29 voltage-dependent K<sup>+</sup>-channels: hKv1.1, hKv1.2, hKv1.3 and hKv1.4. The electrophysiological  
30 assays showed that Pi5 inhibited *Shaker B*, hKv1.1, hKv1.2 and hKv1.3 channels with K<sub>d</sub>=540  
31 nM, K<sub>d</sub>= 92 nM and K<sub>d</sub>= 77 nM, respectively, other studied channels were not affected. Of the  
32 channels tested only hKv1.2 and hKv1.3 were inhibited at 100 nM concentration of Pi6, the  
33 remaining current fractions were 68% and 77%, respectively. Thus, Pi5 and Pi6 are high  
34 nanomolar affinity non-selective blockers of hKv1.2 and hKv1.3 channels.

35

36

37 **KEYWORDS**38 Amino acid sequence; ion-channel; K<sup>+</sup>-channel blocker; *Pandinus imperator*; scorpion toxin

39

40 **1. INTRODUCTION**

41 Most scorpion venoms from the family Buthidae, lethal to humans, contain mainly two types of  
42 toxic peptides: the long-chain Na<sup>+</sup>-channel specific toxins with 60-76 amino acid residues, and  
43 the short-chain peptides with 23-41 amino acid residues, specific for K<sup>+</sup>-channels (Possani et  
44 al.,1999; Garcia et al., 1998). Toxins from scorpion venom specific for K<sup>+</sup>-channel have been  
45 widely described (Tytgat et al., 1999; Rodriguez de la Vega and Possani, 2004; Bartok et al,  
46 2015; Kuzmenkov et al, 2016). The venom from the African scorpion *Pandinus imperator*, from

47 the family Scorpionidae, is different because it is not lethal to humans and instead of having  
48 mammalian specific Na<sup>+</sup>-channel toxins it contains many proteins and peptides with interesting  
49 biological activities, such as imperatoxin activatory (IpTxa) and imperatoxin inhibitory (IpTxi),  
50 both specific for the Ryanodine sensitive Ca<sup>2+</sup>-channels (Zamudio et al., 1997a,b),  
51 phospholipin, a heterodimeric phospholipase (Conde et al., 1999) and scorpine, an antibacterial  
52 and antiparasitic peptide (Conde et al., 2000). Also interesting, more than 10% of its venom is  
53 composed by various peptides that recognize K<sup>+</sup>-channels (Olamendi-Portugal et al. 1996;  
54 Gómez-Lagunas et al., 1996). The first one described was Pi1, which contains four disulfide  
55 bonds instead of three usually found on K<sup>+</sup>-channel specific toxins, at the time when it was  
56 described (Olamendi-Portugal et al., 1996). Then Pi2 and Pi3 were found, which differ only by  
57 one amino acid residue in their primary structure, but have a 17 fold difference of activity,  
58 assayed in *Shaker* B K<sup>+</sup> channels (Gomez-Lagunas et al., 1996). Additionally, Pi4 and Pi7 were  
59 described, the first with a K<sub>d</sub> of 8.2 nM, whereas the second had no activity against the *Shaker*  
60 K<sup>+</sup>-channel (Olamendi-Portugal et al., 1998). The three-dimensional structure (3D) of Pi1 and  
61 Pi4 were determined (Delepierre et al., 1997; Delepierre et al, 1998; Guijarro et al., 2003)  
62 Additionally the 3D structure of Pi7, that lacks a K<sup>+</sup> channel blocking potency, was also solved  
63 (Delepierre et al., 1999) in order to reveal possible differences on the folding pattern of the  
64 peptides. The general 3D folding of Pi7 turned out to be identical to the other known K<sup>+</sup>-channel  
65 specific toxins, however an Arg in position 27 (equivalent to lysine-27 of Charybdotoxin) was  
66 taken as one of the possible differences among these toxins, that would render Pi7 ineffective  
67 against the tested channels. Approximately at the same time, two additional peptides were  
68 identified in this venom, and were called Pi5 and Pi6. The trivial name comes from the  
69 abbreviations of scorpion species (*Pandinus imperator*) and the number of purified peptides, at

70 that time. Systematic nomenclature is now being assigned for both peptides. Pi5 is a new  
71 member of the family  $\alpha$ -KTx. The number of amino acids, disulfide bonds and sequence  
72 similarities indicate that it is the first member of the sub-family 24 (systematic number  $\alpha$ -KTx  
73 24.1). Pi6 belongs to the  $\kappa$ -family, with the systematic number assigned  $\kappa$ -KTx 2.9. Their  
74 structures were not published, because the functional activity of the peptides was not clearly  
75 determined. In this communication we fill this gap and describe both peptides; their primary  
76 structure and their inhibitory potential of several ion channel subtype of the of the Shaker family  
77 including *Shaker B*, Kv1.1-Kv1.4 and on the *Shab* channel.

78

## 79 **2. Material and Methods**

### 80 *2.1 Source of venom*

81 Living scorpions (approximately 100 animals) of the species *Pandinus imperator*, from Gabon  
82 (Africa), were bought from a pet-shop (Pet Supplies Plus, Ann Arbor, Michigan, USA) and kept  
83 alive in the laboratory for several years. This occurred before this species became included on  
84 the CITES list for danger of extinction. The scorpions were very well adapted; grow well and  
85 even reproduced in captivity. The venom from adult animals, at that time, was obtained by  
86 electric stimulation under anesthesia with CO<sub>2</sub>, dissolved in double distilled water and  
87 centrifuged 10,000 g for 15 min. The supernatant was freeze-dried and stored at -20 °C until use.

88

### 89 *2.2 Purification procedure and amino acid sequence determination*

90 The soluble venom was initially fractionated by gel filtration on Sephadex G-50 column. Sub-  
91 fractions were further separated by high performance liquid chromatography (HPLC), using a  
92 C18 reverse-phase column (Vydac, Hysperia, CA) of a Waters 600E HPLC system, equipped

93 with a variable wavelength detector, and a WIPS 712 automatic sample injector, as described  
94 (Olamendi-Portugal et al., 1996).

95 The homogeneity of the purified peptides was confirmed by a step-gradient HPLC (only one  
96 symmetric peak), molecular mass determination on LCQ<sup>DUO</sup> Finnigan mass spectrometer (San  
97 Jose, CA), and by direct Edman degradation using an automatic ProSequencer (Millipore model  
98 6400/6600); Olamendi-Portugal et al., 1996).

99 The primary structure of both peptides Pi5 and Pi6 was determined using native samples,  
100 samples reduced and alkylated with iodoacetic acid, and after digesting alkylated peptides with  
101 enzymes, such as chymotrypsin and *Staphylococcus aureus* endopeptidase V8, from which pure  
102 peptides were obtained by HPLC fractionation, essentially as earlier described (Olamendi-  
103 Portugal et al., 1996; 2016), and used for completion of the entire amino acid sequence.

104 The protein sequence data reported in this paper will appear in the UniProt Knowledgebase  
105 under the accession number C0HKB2 for Pi5 and C0HKB3 for Pi6.

106

107 *2.3 Functional characterization of pure Pi5 and Pi6 on Drosophila Shab and Shaker B K<sup>+</sup>-*  
108 *channels*

109 Physiological assays were initially conducted using the expression of *Shab* and *Shaker B K<sup>+</sup>-*  
110 channels in Sf9 cells. The insect Sf9 cells were kept in culture at 27 °C in Grace's media (Gibco  
111 BRL). The cells were transfected by infecting with a recombinant baculovirus (*Autographa*  
112 *californica* nuclear polyhidrosis virus) containing the cDNA of either *Shab* or *Shaker B K<sup>+</sup>-*  
113 channels, as previously reported (Klaiber et al., 1990; Islas and Sgiworth, 1999). The cells were  
114 used for the experiments two days after the infection.

115 The currents were recorded under whole-cell patch-clamp with an Axopatch 1D (Axon  
116 Instruments INC). Borosilicate glass (KIMAX 51) electrodes were pulled to a 1.5 MOhm  
117 resistance, and used without further treatment. Eighty percent of the series resistance was  
118 electronically compensated. The currents were filtered in line at 5 KHz, and sampled at 100  
119  $\mu$ s/point with DIGIDATA 1322A (Axon Instruments, INC). The solutions used were: external  
120 side (in mM): 145 NaCl, 10 CaCl<sub>2</sub>, 10 HEPES-Na buffer, pH 7.1; internal solution (in mM): 95  
121 KF, 30 KCl, 10 EGTA, 10 HEPES-K buffer, pH 7.1.

122

#### 123 *2.4 Functional characterization of pure Pi5 and Pi6 on four voltage-dependent K<sup>+</sup>-channels*

124 Human peripheral lymphocytes were drawn from healthy volunteers. Mononuclear cells were  
125 isolated using Ficoll-Hypaque density gradient separation technique and were grown in 24-well  
126 culture plates in a 5% CO<sub>2</sub> incubator at 37°C in RPMI 1640 medium supplemented with 10%  
127 fetal calf serum (Sigma-Aldrich), 100  $\mu$ g/ml penicillin, 100  $\mu$ g/ml streptomycin, and 2 mM L-  
128 glutamine (density, 5 x 10<sup>5</sup> cells per ml) for 2 to 5 days. 5, 7.5 or 10  $\mu$ g/ml phytohemagglutinin  
129 A (Sigma-Aldrich) was added to the medium to increase K<sup>+</sup> channel expression. CHO cells were  
130 grown under standard condition as described previously (Bagdany et al., 2005; Corzo et al.,  
131 2008; Grissmer et al., 1994).

132 Vectors encoding the human Kv1.1, Kv1.2 and Kv1.4 channels were expressed in CHO cells  
133 using Lipofectamine 2000 (Invitrogen, Carlsbad, CA, USA), according to the manufacturer's  
134 instructions. hKv1.1 and hKv1.2 genes are coded in pCMV6-GFP plasmid (OriGene  
135 Technologies, Rockville, MD), the vector for hKKv1.4 lacking the N-terminal inactivation  
136 domain was a gift from David Fedida (University of British Columbia, Vancouver, Canada). This  
137 latter gene was transiently co-transfected with a plasmid encoding the green fluorescence protein

138 (GFP). Currents were recorded 24 h after transfection. GFP positive transfectants were identified  
139 in a Nikon TE2000U fluorescence microscope and used for current recordings (>70% success  
140 rate for co-transfection). For the measurements of hKv1.3 currents activated lymphocytes were  
141 used (Bartok et al., 2014).

142 Measurements were carried out using whole-cell patch-clamp recordings using Multiclamp 700B  
143 amplifier and Axon Digidata 1440 digitizer (Molecular Devices, Sunnyvale, CA). Micropipettes  
144 were pulled from GC 150 F-15 borosilicate capillaries (Harvard Apparatus Kent, UK) resulting  
145 in 3- to 5-M $\Omega$  resistance in the bath solution. The extracellular solution consisted of 145 mM  
146 NaCl, 5 mM KCl, 1 mM MgCl<sub>2</sub>, 2.5 mM CaCl<sub>2</sub>, 5.5 mM glucose, 10 mM HEPES, pH 7.35. Bath  
147 solutions were supplemented with 0.1 mg/ml BSA when toxins were dissolved. The osmolarity  
148 of the extracellular solutions was between 302 and 308 mOsM/L. The pipette filling solution  
149 contained 140 mM KF, 2 mM MgCl<sub>2</sub>, 1 mM CaCl<sub>2</sub>, 10 mM HEPES and 11 mM EGTA, pH 7.22.  
150 The osmolarity of the intracellular solutions was 295 mOsM/L.

151 Whole cell currents were elicited using by voltage steps to +50 mV for variable durations,  
152 ranging between 15 ms to 500 ms depending on the channel type, from a holding potential of -  
153 100 mV every 15 s. The pClamp10 software package was used to acquire and analyze the data.  
154 Current traces were lowpass-filtered by the analog four-pole Bessel filters of the amplifiers. The  
155 sampling frequency was 2-50 kHz, at least twice the filter cut-off frequency. The effect of the  
156 toxins in a given concentration was determined as remaining current fraction ( $RF = I/I_0$ , where  $I_0$   
157 is the peak current in the absence of the toxin and  $I$  is the peak current at equilibrium block at a  
158 given toxin concentration). The  $K_d$  was determined from the double reciprocal plot of the  
159 blocked fraction of the current ( $B=1-RF$ ) where  $1/B$  was plotted against the reciprocal of the



160 toxin concentration ( $1/C$ ). Fitting a straight line to the data points gave  $K_d$  as the slope of the line  
161 ( $1/B=(K_d*1/C)+1$ ). The fit assumed 1:1 stoichiometry for the toxin-channel interaction.

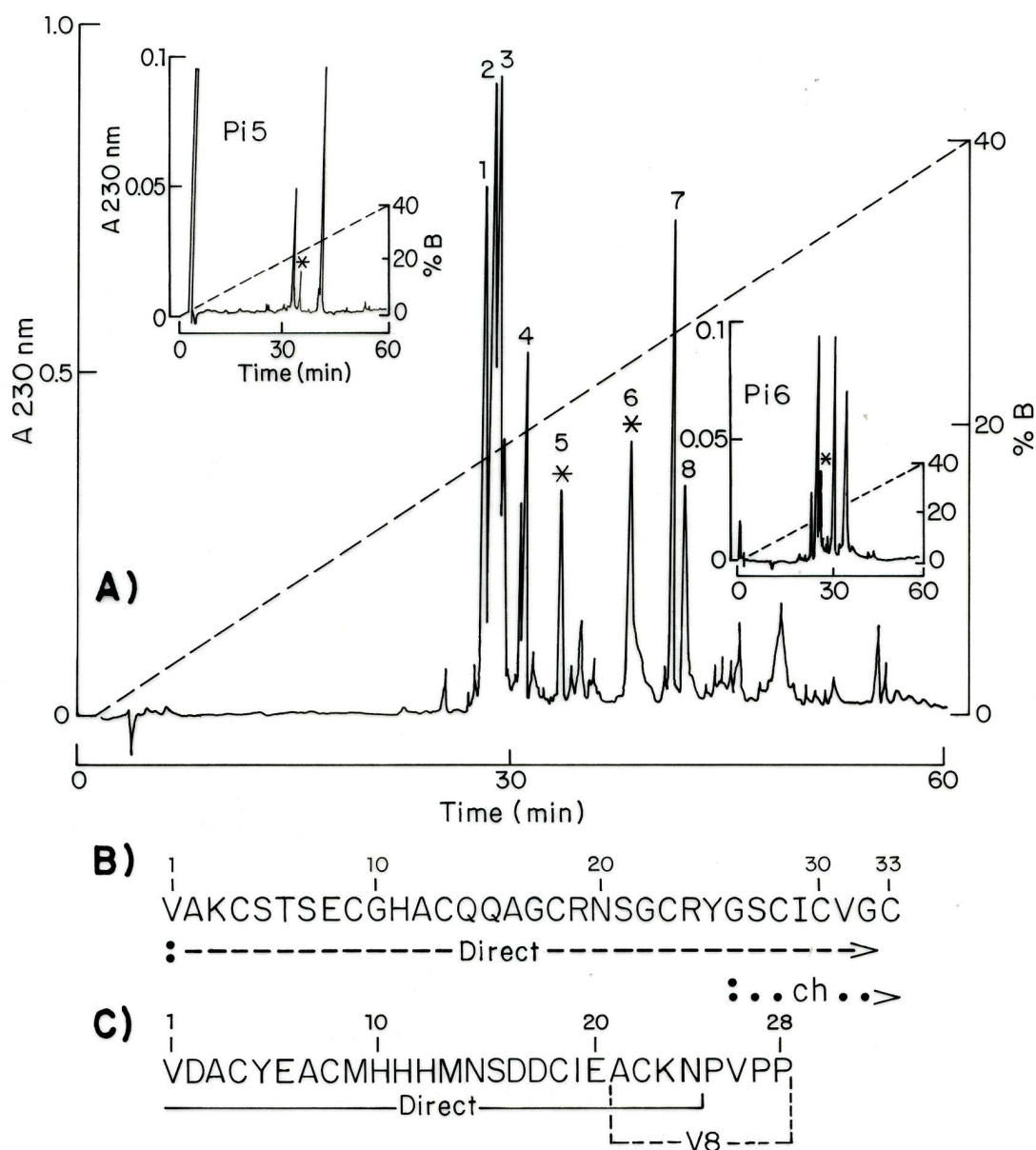
162

### 163 **3. Results and Discussion**

#### 164 *3.1 Purification and amino acid sequencing determination*

165 After separation of the whole soluble venom by gel filtration into Sephadex G-50 column, as  
166 described earlier (Olamendi-Portugal et al. 1996), fraction III containing the peptides of interest  
167 was separated by HPLC. Several batches of fraction III (0.5 mg of protein content) was separated  
168 independently, given always the same profile. Figure 1A shows the results obtained. Eight sub-  
169 fractions were selected for further purification and characterization. Fractions 1 to 4 of Fig.1A  
170 were characterized as Pi1 to Pi4, and fraction 7 as Pi7 (Olamendi-Portugal et al., 1998;  
171 Delepierre et al., 1999). Components labeled 5 and 6 (marked with asterisks) were used for  
172 sequence determination, and named Pi5 and Pi6. The amino acid sequence of Pi5 is shown in  
173 Fig.1B. Native peptide and the same peptide in its iodoacetic alkylated format permitted the  
174 identification of the first 32 amino acids; the last residue was obtained after sequencing the  
175 peptide labeled “Ch”, which overlaps with residues of the C-terminal region of the peptide,  
176 completing the sequence. This peptide was obtained after digesting 50  $\mu$ g of the reduced and  
177 alkylated peptide by HPLC (Fig.1A, left side labeled Pi5). The peptide marked with asterisk  
178 gave the sequence from 26-33. The experimental determined molecular weight (average  
179 molecular mass) of the native Pi5 peptide was 3334.00 Da and the theoretically expected was  
180 3334.81 Da, confirming the full sequence, within the experimental error of the mass  
181 spectrometer used for this analysis. The peptide contains 8 cysteines that are forming 4 disulfide  
182 bonds. Using the same procedure the amino acid sequence of peptide Pi6 was determined as

183 shown in Fig.1C. The first 24 amino acid residues were identified by direct Edman degradation  
184 of native and native-alkylated samples. Alkylation of cysteines was essential for the correct  
185 identification of the thiol containing amino acids. The complete sequence was obtained after  
186 digesting 50  $\mu$ g of peptide Pi6 with endopeptidase V8, whose separation profile on HPLC is  
187 shown on the right inset panel of Fig.1A, labeled Pi6 and marked with asterisk. This peptide  
188 gave the sequence from amino acid Ala21 to Pro28. The molecular weight experimentally  
189 determined (average molecular mass) for this peptide was 3126.5 Da and the theoretical  
190 molecular weight was 3127.2, within the experimental error of the spectrometer used for this  
191 analysis. This peptide has 4 cysteines forming only two disulfide bonds.



192

193 **Figure 1: Purification and amino acid sequence of Pi5 and Pi6**

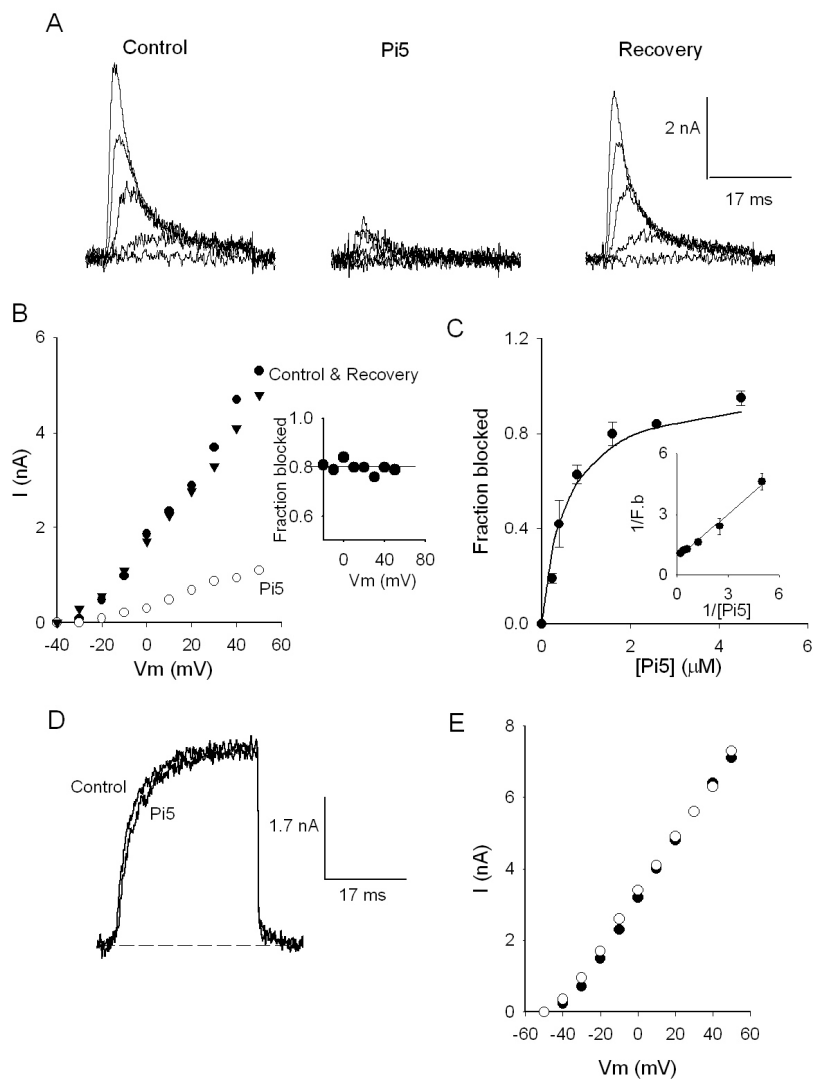
194 A. Fraction III from Sephadex G-50 column (0.5 mg) was separated by HPLC using an  
 195 analytical C18 reverse-phase column (4.6 x 250 mm), with a linear gradient from solution A  
 196 (0.12% trifluoacetic acid –TFA- in water) to 40% solution B (0.10% TFA in acetonitrile). Sub-  
 197 fraction 5 (labeled with asterisk) was homogeneous Pi5, which was digested with chymotrypsin  
 198 and separated again in the same conditions, as indicated in the inset figure labeled Pi5. The

199 asterisk indicates the peptide whose sequence allowed completion of the amino acid sequence  
200 shown in letter B, from position 26 to 33 (underlabeled with .Ch.). Similarly, the sub-fraction 6  
201 (labeled with asterisk) was the homogeneous peptide Pi6, which was digested with Protease V8  
202 from *Staphylococcus aureus*, and separated in the same conditions, as indicated in the insert  
203 labeled Pi6. The labeled peptide with asterisk was sequenced and permitted completion of the  
204 sequence from amino acids in position 21 to 28 (underlined .V8.). Letters B and C show the full  
205 amino acid sequence for both peptides, where “Direct” means amino acid sequence obtained  
206 with a reduced and alkylated sample of each peptide.

207

### 208 3.2 Effects of Pi5 and Pi6 on *Shab* and *Shaker* K<sup>+</sup>-channels

209 Fig. 2A demonstrates that Pi5 is a toxin that reversibly blocks, *Drosophila Shaker B* K<sup>+</sup> channels  
210 with low affinity. The left panel presents a family of control K<sup>+</sup> currents (see Figure legend),  
211 note that upon addition of 1.5 μM Pi5, to the extracellular solution, the size of I<sub>K</sub> was drastically  
212 reduced (~80%, middle panel). Inhibition was fully reversed by washing the cell with the control  
213 solution (right panel). Experiments repeated at lower Pi5 concentrations show that Pi5 simply  
214 scales down the currents without changing its kinetics. The I-V relationship of the traces shown  
215 in Fig. 2B demonstrates that, as commonly found with Kv channel blocker toxins, the fraction of  
216 the channels blocked by Pi5 is independent of the applied voltage. The fit to the dose-response  
217 relationship resulted in a K<sub>d</sub> of 540 nM (Fig. 2C) with Hill coefficient close to 1 indicating that  
218 the Pi5 blocks *Shaker* channels with a 1:1 stoichiometry. The double reciprocal plot (Fig. 2 C  
219 inset) could be well-fit using linear regression (r=0.995), the K<sub>d</sub> values obtained by the two  
220 methods were comparable. In contrast to the above observations, addition of 1.5 μM Pi5 to the  
221 extracellular solution did not inhibit significantly *Drosophila Shab* K<sup>+</sup> channels (Figures 2D and  
222 2E). Pi6 on the other hand did not inhibit the either *Shaker B* or *Shab* (See Supplementary Figure  
223 1).



224

225 **Figure 2: Effect of Pi5 on *Drosophila* K<sup>+</sup> channels**

226 (A) K<sup>+</sup> currents through *dShaker B* channels. K<sup>+</sup>-currents were elicited every 15-sec by 30-ms  
 227 pulses from -20 to +60 mV applied in 10 mV increments from a holding potential of -80 mV,

228 before (left panel, labeled Control), during (middle panel, labeled Pi5) and after (labeled

229 Recovery) the addition of 1.5 μM Pi5 to the external solution. (B) Current-Voltage relationship

230 of the traces in A: closed circles: control I<sub>K</sub>, open symbols: I<sub>K</sub> with 1.5 μM Pi5 in the external

231 solution, closed triangles: I<sub>K</sub> after washing the cell with the control solution. The inset shows

232 that the block (1.5 μM Pi5) is not voltage dependent. (C) Fractional block vs. [Pi5], the fractional

233 block (F.b) was calculated as  $F.b = 1 - (I/I_0)$ , where I<sub>0</sub> and I are the peak current in the control and

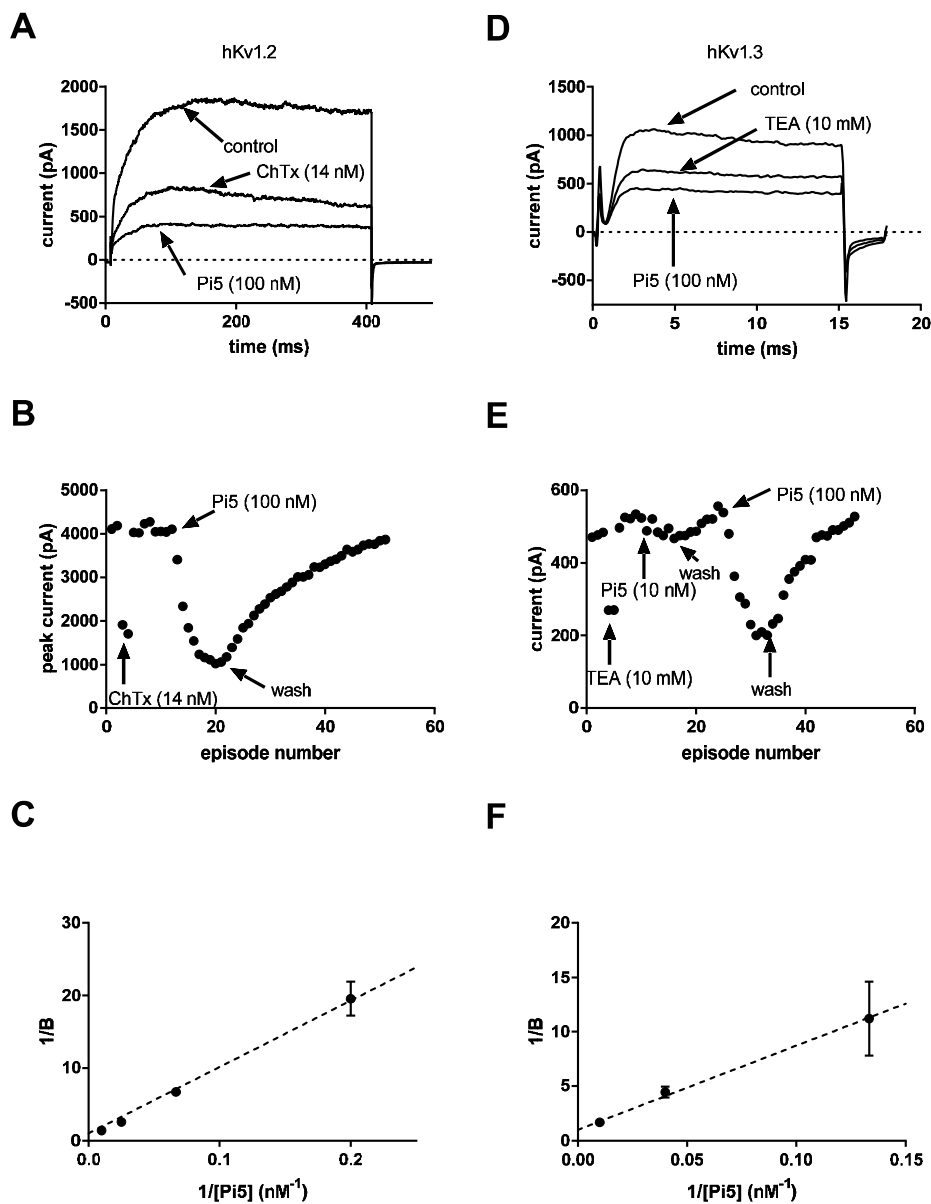
234 in the presence of Pi5, respectively. The line is the least squares fit of the points with the  
235 Michaelis-Menten equation, with  $K_d = 540$  nM. The inset shows the expected linear double-  
236 reciprocal plot of the points ( $r = 0.995$ ). (D)  $K^+$  currents through dShab channels. The figure  
237 shows two superimposed currents evoked by a 30mV/30ms pulse applied from -80 mV, before  
238 and during addition of 1.5  $\mu$ M Pi5, as indicated. (E) Current-voltage relationship before and in  
239 the presence of 1.5  $\mu$ M Pi5 from traces as in D. There was no blockage.

240

### 241 3.3 Effects of Pi5 and Pi6 on hKv1.1, hKv1.2, hKv1.3 and hKv1.4 channels.

242 Based on the similarity of Pi5 and Pi6 with other known  $\alpha$ -KTx toxins (see also below) and the  
243 literature available for the selectivity of similar peptides ((Camargos et al., 2011; Gomez  
244 Lagunas et al., 1997; Mouhat et al., 2004; Peter et al., 2000)), the following *Shaker*-related  
245 human ion channels were selected for the study: Kv1.1, Kv1.2, Kv1.3 and Kv1.4. These channels  
246 were either expressed heterologously in CHO cells (Kv1.1, Kv1.2 and Kv1.4) or were recorded  
247 in human peripheral blood lymphocytes where the dominant voltage-gated  $K^+$  channel is Kv1.3.  
248 Our recording condition (no  $Ca^{2+}$  in the pipette to evoke  $Ca^{2+}$ -activated  $K^+$  channels) and the  
249 stimulation of the  $K^+$  channel expression (activation of the cells by PHA, see methods) ensured  
250 that the voltage-gated current recorded in these cells is a  $K^+$  current through Kv1.3 (Peter et al.,  
251 2001). The toxins were applied using a custom built microperfusion system with a very small  
252 perfusion rate (200  $\mu$ L/min). At this perfusion rate the speed and the completeness of the  
253 solution exchange had to be tested repeatedly. The positive controls for perfusion were either  
254 quick and fully reversible blockers of the channels (e.g. TEA for Kv1.3 and Kv1.1 and ChTx for  
255 Kv1.2 (Bartok et al., 2014)) or the recording chamber was perfused with a modified bath solution  
256 containing 150 mM  $K^+$  and reduction of the peak currents was used as an indicator of the  
257 solution exchange.

258 The effect of Pi5 on the whole cell current carried by hKv1.2 channels is shown in Fig. 3A. The  
259 figure shows that Pi5 in 100 nM concentration inhibits ~80% of the whole-cell current upon  
260 reaching block equilibrium (perfusion of the recording chamber with ChTx was used as a  
261 positive control of the solution exchange). The comparison of the currents recorded in the  
262 presence and absence of the blocker indicates that the kinetics of the whole-cell currents are  
263 unaffected by the application of Pi5. The block of the hKv1.2 channels was fully but slowly  
264 reversible by perfusing the recording solution with toxin-free extracellular solution (Fig. 3B,  
265 indicated by the arrow labeled wash). The interepisode time during the recording was 15s and the  
266 wash-out is complete in ~50 episodes which correspond to ~12-13 min. The kinetics of the  
267 recovery from block followed a single exponential time-course (fit not shown) with a time  
268 constant of  $245 \pm 26$  s ( $n=3$ ). The limited amount of the purified peptides allowed the dose-  
269 response relationship to be determined over a limited range of Pi5 concentrations, between 5 and  
270 100 nM (Fig. 3C). The best fit linear regression to the double reciprocal plot shown in Fig. 3C  
271 resulted in a  $K_d$  of 92 nM ( $R^2=0.99$ ). Pi5 inhibited the hKv1.3 current expressed in human T  
272 cells with similar potency, the remaining current fractions of hKv1.2 and hKv1.3 currents were  
273  $0.29 \pm 0.03$  ( $n=4$ ) and  $0.39 \pm 0.02$  ( $n=5$ ), respectively, in the presence of 100 nM Pi5. Fig. 3D  
274 shows the raw current traces in the presence and absence of 100 nM Pi5, 10 mM TEA was used  
275 as a positive control for solution exchange. The kinetics of the blocked hKv1.3 current did not  
276  
277



278

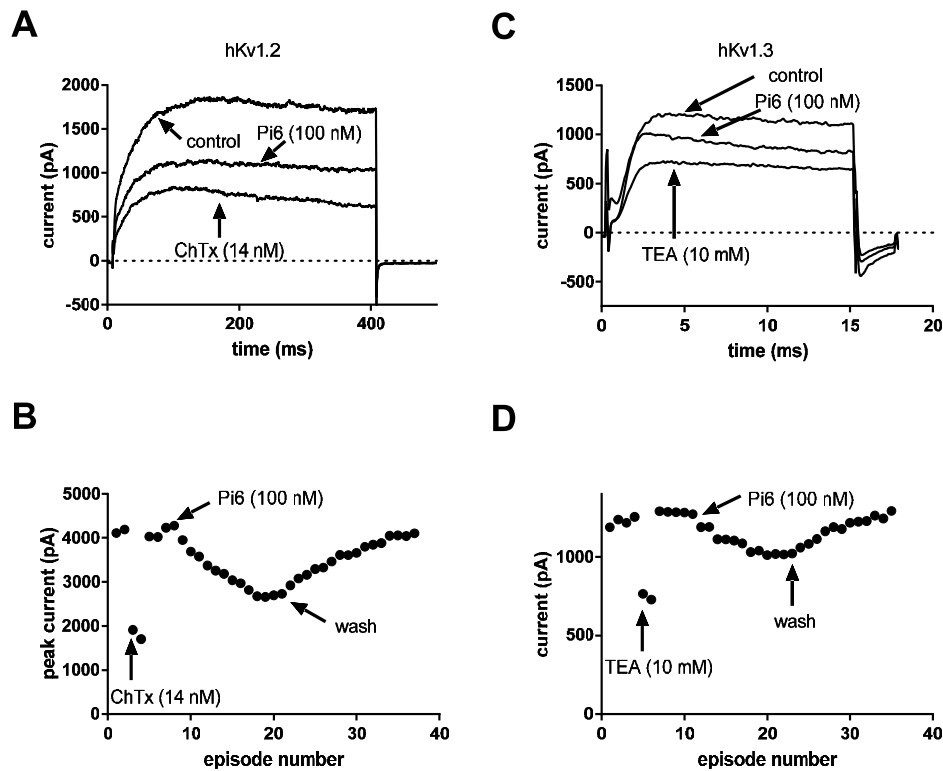
279

### 280 **Figure 3: Block of Kv1.2 and Kv1.3 channels by Pi5**

281 A) Whole-cell potassium currents through hKv1.2 channels were evoked from a transiently  
 282 transfected CHO cells in response to depolarizing pulses to +50 mV from a holding potential of -  
 283 100 mV every 15s. The current traces were recorded in the absence of the toxins (control,  
 284 indicated by arrow), after equilibration of the block in the presence of Pi5 (indicated by arrow) in



285 100 nM concentration. Charybdotoxin (ChTx, arrow, 14 nM) was used as a positive control. B)  
286 Development of and recovery from block of Kv1.2 by Pi5. Peak currents were determined during  
287 repeated depolarizations to +50 mV, arrows indicate the start of the bath perfusion with 100 nM  
288 Pi5 or with the toxin-free bath solution (labeled “wash”). C) Double-reciprocal plot of the dose-  
289 response of Pi5 on hKv1.2. See methods for details. The linear regression ( $1/B=(Kd*1/C)+1$ )  
290 resulted in a Kd of 92 nM ( $R^2=0.99$ ). D) Whole-cell potassium currents through hKv1.3 channels  
291 were evoked from in activated human peripheral lymphocytes in response to depolarizing pulses  
292 to +50 mV from a holding potential of -100 mV every 15s. The current traces were recorded in  
293 the absence of the toxins (control, indicated by arrow), after equilibration of the block in the  
294 presence of Pi5 in 100 nM concentration (arrow). Tetraethylammonium (TEA, arrow, 10 mM)  
295 was used as a positive control. D) Development of and recovery from block of Kv1.3 by Pi5.  
296 Peak currents were determined during repeated depolarizations to +50 mV, arrows indicate the  
297 start of the bath perfusion with 10 nM Pi5 or 100 nM Pi5 or the toxin-free bath solution (arrow  
298 labeled wash). E) Double-reciprocal plot of the dose-response of Pi5 on hKv1.3. See methods  
299 for details. The linear regression ( $1/B=(Kd*1/C)+1$ ) resulted in a Kd of 77 nM ( $R^2=0.99$ ).  
300  
301 differ from the control one, similar to the results obtained for the inhibition of the hKv1.2  
302 currents. The block of the Kv1.3 current by Pi5 was fully reversible, as indicated by the full  
303 recovery of the peak currents following the application of Pi5 in 10 nM and 100 nM  
304 concentrations (Fig. 3 E, indicated by arrows). The wash-out of the peptide was complete in ~15  
305 episodes corresponding to ~225 s. The kinetics of the recovery from block followed a single  
306 exponential time-course (fit not shown) with a time constant of  $80\pm 6$  s ( $n=4$ ). The best fit linear  
307 regression to the double reciprocal plot shown in Fig. 3F resulted in a Kd of 77 nM ( $R^2=0.99$ ).  
308 The same set of experiments was repeated using Pi6 and the effect of this peptide at 100 nM  
309 concentration was studied on the hKv1.2 and hKv1.3 currents. Panels A and C of Fig. 4 show the  
310 raw current traces whereas panels B and D show the change in the peak currents upon  
311 application and wash-out of Pi6 when cells expressing hKv1.2 (A, B) or hKv1.3 (C,D) channels



312

313

#### 314 **Figure 4: Block of Kv1.2 and Kv1.3 channels by Pi6**

315 A) Whole-cell potassium currents through hKv1.2 channels were evoked from a transiently  
 316 transfected CHO cells in response to depolarizing pulses to +50 mV from a holding potential of -  
 317 100 mV every 15s. The current traces were recorded in the absence of the toxins (control,  
 318 indicated by arrow), after equilibration of the block in the presence of Pi6 (indicated by arrow) in  
 319 100 nM concentration. Charybdotoxin (ChTx, arrow, 14 nM) was used as a positive control. B)  
 320 Development of and recovery from block of Kv1.2 by Pi6. Peak currents were determined during  
 321 repeated depolarizations to +50 mV, arrows indicate the start of the bath perfusion with 100 nM  
 322 Pi6 or with the toxin-free bath solution (labeled “wash”). C) Whole-cell potassium currents  
 323 through hKv1.3 channels were evoked from in activated human peripheral lymphocytes in  
 324 response to depolarizing pulses to +50 mV from a holding potential of -100 mV every 15s. The  
 325 current traces were recorded in the absence of the toxins (control, indicated by arrow), after  
 326 equilibration of the block in the presence of Pi6 in 100 nM concentration (arrow).

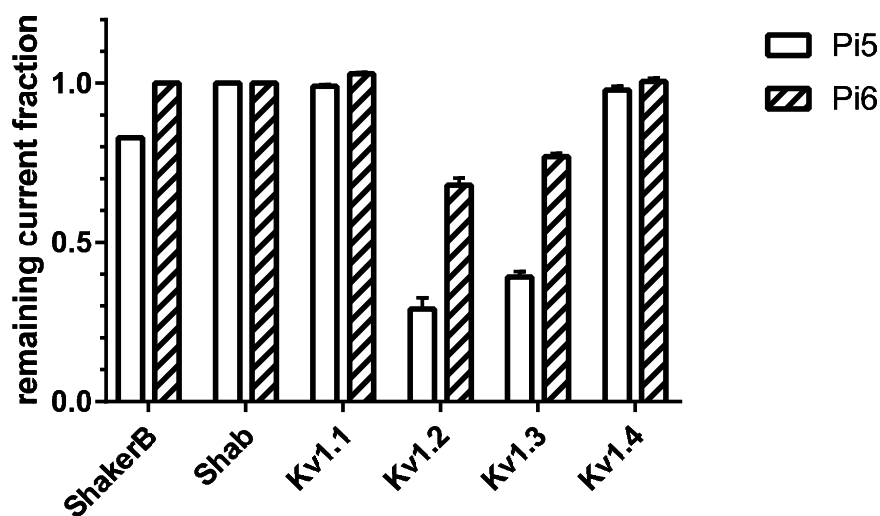
327 Tetraethylammonium (TEA, arrow, 10 mM) was used as a positive control. D) Development of  
328 and recovery from block of Kv1.3 by Pi6. Peak currents were determined during repeated  
329 depolarizations to +50 mV, arrows indicate the start of the bath perfusion with 100 nM Pi6 or the  
330 toxin-free bath solution (arrow labeled wash).

331  
332 in whole-cell patch-clamp. The raw traces recorded at +50 mV test potential show that Pi6 is a  
333 low affinity blocker of both hKv1.2 and hKv1.3. The statistical analysis of the remaining current  
334 fractions upon reaching block equilibrium resulted in  $RF = 0.68 \pm 0.02$  (n=5) and  $RF = 0.77 \pm$   
335  $0.01$  (n=4) for hKv1.2 and hKv1.3 currents, respectively. The recovery from the block of both  
336 hKv1.2 (B) and hKv1.3 (D) was complete in ~300 s. The amount of the purified peptides was  
337 not sufficient to obtain the dose-response relationship of inhibitions for either hKv1.3 or hKv1.3.  
338 Supplementary Figure 2 shows on the other hand, that neither Pi5 nor Pi6 inhibits hKv1.1 or  
339 hKv1.4 channels in 100 nM concentration. To obtain a more precise determination of the peak  
340 currents in hKv1.4 expressing cells we transfected the N-terminal inactivation particle deleted  
341 hKv1.4 construct (Kv1.4-ΔN). Supplementary Figure 2A and Supplementary Figure 2C show  
342 hKv1.1 and hKv1.4 currents, respectively, recorded before application of the peptides and after  
343 the 10<sup>th</sup> pulse in the toxin-containing solution. The overlapping current traces indicate the lack of  
344 block, similarly to the constant peak currents regardless of the presence or absence of the  
345 peptides shown in Supplementary Figure 2B and Supplementary Figure 2D.

346 The effect of Pi5 and Pi6 in 100 nM concentration on the ion channels included in this study is  
347 summarized in Fig. 5. The data show that these peptides inhibit significantly, the human Kv1.2  
348 and Kv1.3 channels and that Pi5 is slightly more potent blocker of these channels than Pi6.

349 Furthermore, Pi5 also inhibits Shaker B channels with low affinity.

350



351

### 352 **Figure 5: Selectivity profile of Pi5 and Pi6**

353 A) Bars indicate the remaining current fractions at equilibrium block of the indicated channels by  
 354 100 nM Pi5 (empty bars) or 100 nM Pi6 (hatched bars). For the expression systems, solutions  
 355 and voltage protocols see Materials and Methods and Figs 2-4 and supplementary Fig. 2. Error  
 356 bars indicate SEM (n=3-6).

357

### 358 *3.4 Comparative analysis of amino acid sequence of the Pi toxins*

359 Fig.6 shows the amino acid sequence of K<sup>+</sup>-channel blocking peptides isolated from *Pandinus*  
 360 *imperator* venom. The similarities of these sequences are relatively low (39 to 55% identity  
 361 taking Pi1 as the reference), and it is practically nonexistent for Pi6 (14%). The peptides Pi1, Pi4,  
 362 Pi5 and Pi7 have four disulfide bonds; Pi2 and Pi3 have 3 and Pi6 only 2. The longest ones are  
 363 Pi4 and Pi7, containing 37 amino acid residues, whereas Pi6 has only 28. The conserved residues  
 364 are shaded shown, mainly cysteines. Pi2 and Pi3 differ only by one amino acid in position 7,  
 365 which is a Proline for Pi2 and Glutamic acid for Pi3.

366 The general pattern of ion channel inhibition by Pi5 matches to those of the *Pandinus imperator*  
 367 toxins, these peptides inhibit Kv1.2 and Kv1.3 channels with nM-pM affinities without

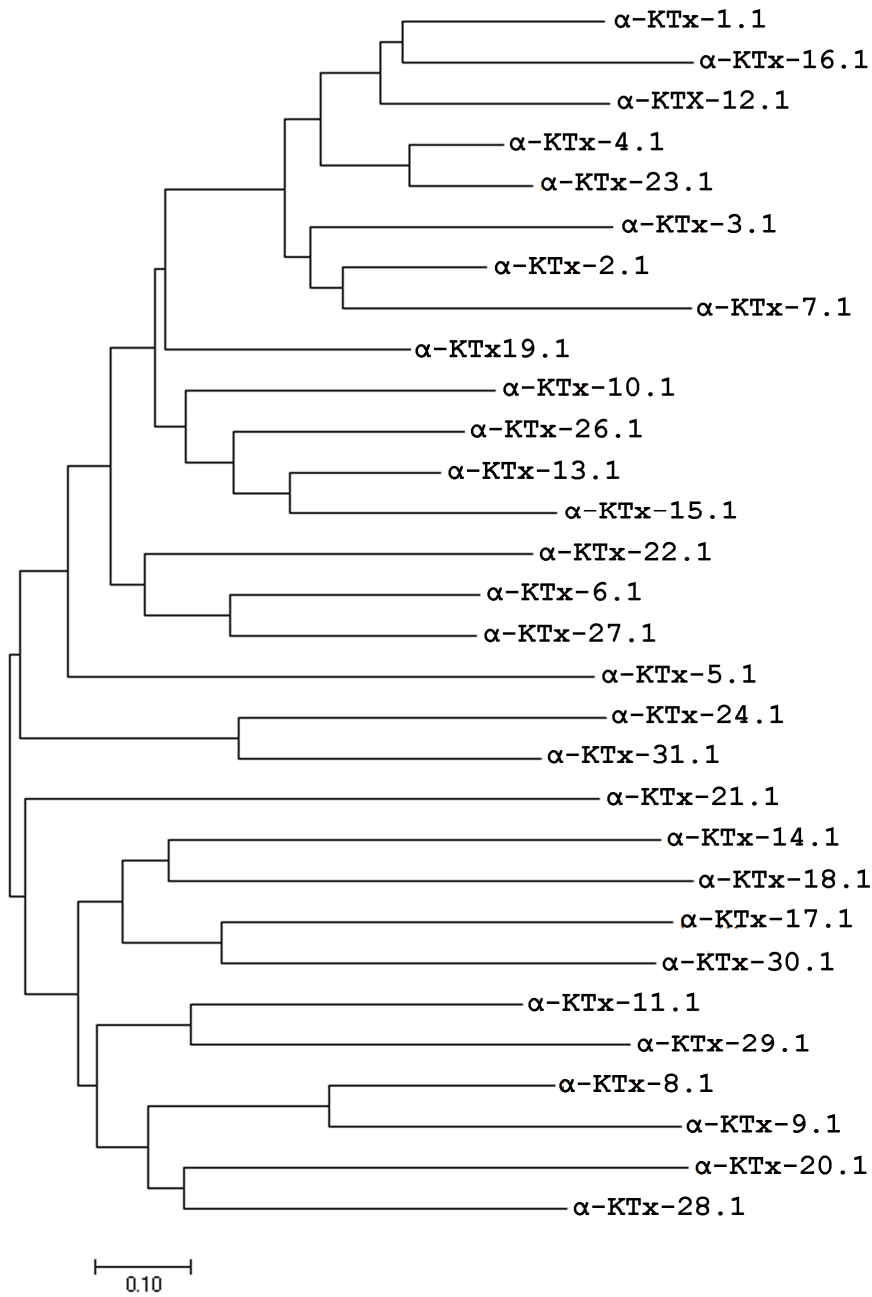
368  
 369 significant selectivity for either of the channels (Fig. 6). Pi6, on the other hands, is different from  
 370 the other members since it does not inhibit *Shaker*, and has very low affinity to Kv1.2 and Kv1.3.  
 371 These properties of Pi6 match to the systemic nomenclature (see below).

Amino acid sequence	% Iden.	Ion channels inhibited (Kd, ref)
Pi1 --LVKCRGTSDCGRPCQQQTGCPNS-KCINRMCKCYGC-	100	Kv1.2 (1.3 nM, (1)), Kv1.3 (11.7 nM, (2)), <i>Shaker</i> (32 nM, (3))
Pi2 --TISCINPKQCYPHCKKETGYFNA-KCMNRKCKCFGR-	52	Kv1.2 (32 pM, (4)), Kv1.3 (44 pM, (5)), <i>Shaker</i> (8.2 nM, (6))
Pi3 --TISCINEKQCYPHCKKETGYFNA-KCMNRKCKCFGR-	52	Kv1.3 (795 pM, (5)), <i>Shaker</i> (140 nM, (6))
Pi4 IEAIRCGGSRDCYRRCQKRTGCPNA-KCINKTCRCYGCS	39	Kv1.2 (8 pM, (7)), <i>Shaker</i> (8 nM, (8))
Pi7 DEAIRCTGTDCYIPCRYITGCFNS-RCINKSKCKYGCT	44	not known
Cons.1-----C-----C---C---TG---N---C-N---CRC-G--		
Pi5 --VAKCSTSE-CGHACQQA-GCRNS-GCRYGSCICVGC-	55	Kv1.2 (92 nM), Kv1.3 (77 nM), <i>Shaker</i> (540 nM)
Pi7 --VDACY--EACMHHMNSDDCIEA--CKNPVPP-----	14	Kv1.2 (>>100 nM), Kv1.3 (>>100 nM)
Cons.2--V--C---E-C-H-----C-----C-----		

372  
 373 **Figure 6: Comparative sequences of *Pandinus imperator* toxins**  
 374 Amino acid sequences of the K<sup>+</sup>-channel peptides isolated from *Pandinus imperator* and  
 375 percentage of identity (Iden.) compared to Pi1. Cons.1 and Cons.2 stand for consensus on the  
 376 relative positions of the cysteine residues in Pi1-Pi4, Pi7 and Pi5, Pi6, respectively. Amino acids  
 377 in identical positions are highlighted in gray. References (ref) in this figure correspond to: (1)  
 378 (Mouhat et al., 2004), (2) (Peter et al., 2000), (3) (Gomez Lagunas et al., 1997), (4) (Rogowski et  
 379 al., 1996), (5) (Peter et al., 2001), (6) (Gomez-Lagunas et al., 1996), (7) (M'Barek et al., 2003)  
 380 and (8) (Olamendi-Portugal et al., 1998).

381  
 382 The databank KALIUM (see reference Kuzmenkov et al., 2016), by November 2016 listed 174  
 383 distinct amino acid sequence belonging to  $\alpha$ ,  $\beta$ ,  $\delta$ ,  $\kappa$  and  $\lambda$  families, from which Pi5 and Pi6  
 384 belong to  $\alpha$  and  $\kappa$  families, respectively. When this manuscript was been prepared another new  
 385 sub-family ( $\alpha$ -KTx 31.1) was described (ElFessi-Magouri et al., 2016). Pi5 is the first example of  
 386 a new subfamily, and the systematic number assigned was  $\alpha$ -KTx 24.1 (See Supplementary  
 387 Fig.3). We found that the subfamily number 25 was never used. New coming sequences, that  
 388 according to the initial proposed nomenclature (Tytgat et al., 1999) justifies the assignation of

389 new member for systematic classification, should use the number 25. The physiological effects  
 390 of Pi5 described here, certainly justifies including this sequence as a *bona fide*  $\alpha$ -KTx peptide.  
 391 This classification was supported in addition by the phylogenetic analysis conducted, using the  
 392 number one sequence of each subfamily described until now.



393

394 **Figure 7: Unrooted phylogenetic tree of  $\alpha$ -KTx**

395 A multiple sequence alignment of 30 sequences were retrieved from public databases, literature  
 396 or unpublished results from our laboratory. The evolutionary history was inferred using the  
 397 Neighbor-Joining method. The tree is drawn to scale, with branch lengths in the same units as  
 398 those of the evolutionary distances used to infer the phylogenetic tree. The evolutionary  
 399 distances were computed using the Poisson correction method and are in the units of the number  
 400 of amino acid substitutions per site. Evolutionary analyses were conducted in MEGA7.

401  
 402  $\kappa$ -KTx2.1 OmTx1 -DPCYEVC LQQHGNVKECEEACKHPVE  
 403  $\kappa$ -KTx2.2 OmTx2 -DPCYEVC LQQHGNVKECEEACKHPVEY  
 404  $\kappa$ -KTx2.3 OmTx3 NDPCEEVCLQHTGNVKACEEACQ-----  
 405  $\kappa$ -KTx2.4 OmTx4 -DPCYEVC LQQHGNVKECEEACKHP---  
 406  $\kappa$ -KTx2.5 OcyC8 YDACVNACLEHHPNVRECEEACKNPVPP  
 407  $\kappa$ -KTx2.6 OcyC9 FPPCVEVCVQHTGNVKECEAACGE-----  
 408  $\kappa$ -KTx2.7 HSP053C.1 -NACIEVC LQHTGNPAECDKACDK----  
 409  $\kappa$ -KTx2.8 HSP053C.2 GNACIEVC LQHTGNPAECDKPCDK----  
 410  $\kappa$ -KTx2.9 Pi6 VDACYEACMHHHMNSDDCIEACKNPVPP

411

412 **Figure 8: Amino acid sequence of the family  $\kappa$ -KTx 2**

413 Pi6 is the number 9 of this subfamily.

414

415 Relatively limited information is available for the inhibition of  $K^+$  channels by  $\kappa$ -KTx peptides  
 416 albeit the family consists of 9 members now. The only peptide studied in this group so far is  $\kappa$ -  
 417 KTx 2.5 (OcyC8) where a low affinity inhibition of Kv1.1 ( $K_d=217 \mu\text{M}$ ) and Kv1.4 ( $K_d=71$   
 418  $\mu\text{M}$ ) were reported earlier (Camargos et al., 2011). These peptides do not conform to the general  
 419 pattern of the peptides inhibiting  $K^+$  channels with high affinity, Pi6 has less cysteines to make  
 420 disulfide bridges and the 2 antiparallel beta sheets plus the  $\alpha$  helix cannot be assigned to Pi6.  
 421 Regardless, it is very interesting that Pi6 does inhibit (albeit with low affinity) voltage gated  $K^+$   
 422 channels (this communication) which might be related to an unspecific effect of charged amino  
 423 acid residues. Thus, the real effect of this peptide remains to be clarified, if any.

424 In summary, we have identified and biochemically characterized two novel peptides from  
425 *Pandinus imperator*, and assigned the systemic names of  $\alpha$ -KTx 24.1 (Pi5) and  $\kappa$ -KTx 2.9 (Pi6)  
426 to them. Due to the relatively low affinity of Kv1.2 or kv1.3 inhibition the applicability of these  
427 peptides as research or therapeutic purposes is unlikely. On the other hand, our results contribute  
428 to the description of the biodiversity of the scorpion peptides regarding their primary structure  
429 and biological function.

430

#### 431 **Ethical Statement**

432 This manuscript does not include any studies using human subjects. Authors declare that the  
433 described work has not been published previously. All authors approve this manuscript.

434

#### 435 **Conflict of interest**

436 The authors do not have any conflicts of interest to disclose.

437

#### 438 **Acknowledgements**

439 Supported in part by grant IN203416 from DGAPA-UNAM to LDP, and by GINOP-2.3.2-15-  
440 2016-00015 project (GP). The project is co-financed by the European Union and the European  
441 Regional Development Fund.

442

#### 443 **REFERENCES**

444 Bagdany, M., C.V. Batista, N.A. Valdez-Cruz, S. Somodi, R.C. Rodriguez de la Vega, A.F.

445 Licea, Z. Varga, R. Gaspar, L.D. Possani, and G. Panyi. 2005. Anuroctoxin, a new



- 446 scorpion toxin of the alpha-KTx 6 subfamily, is highly selective for Kv1.3 over IKCa1  
447 ion channels of human T lymphocytes. *Mol.Pharmacol.* 67:1034-1044.
- 448 Bartok, A., A. Toth, S. Somodi, T.G. Szanto, P. Hajdu, G. Panyi, and Z. Varga. 2014.  
449 Margatoxin is a non-selective inhibitor of human Kv1.3 K<sup>+</sup> channels. *Toxicon* 87:6-16.
- 450 Bartok, A., Panyi, G., Varga, Z., 2015. Potassium channel blocking peptide toxins from scorpion  
451 venom, in Possani, L.D., Schwartz, E.F., Rodríguez de la Vega (Eds.), *Scorpion venoms*,  
452 Springer, Heidelberg, 493-527.
- 453 Camargos, T.S., R. Restano-Cassulini, L.D. Possani, S. Peigneur, J. Tytgat, C.A. Schwartz, E.M.  
454 Alves, S.M. de Freitas, and E.F. Schwartz. 2011. The new kappa-KTx 2.5 from the  
455 scorpion *Opisthacanthus cayaporum*. *Peptides* 32:1509-1517.
- 456 Conde, R., Zamudio, F.Z., Becerril, B. y Possani, L.D., 1999. Phospholipin, a novel  
457 heterodimeric phospholipase A2 from *Pandinus imperator* scorpion venom. *FEBS Lett.*  
458 460, 447-450.
- 459 Conde, R., Zamudio, F.Z., Rodríguez, M.H., and Possani, L.D., 2000. Scorpine, an anti-malaria  
460 and anti-bacterial agent purified from scorpion venom. *FEBS Lett.* 471, 165-168
- 461 Corzo, G., F. Papp, Z. Varga, O. Barraza, P.G. Espino-Solis, R.C. Rodriguez de la Vega, R.  
462 Gaspar, G. Panyi, and L.D. Possani. 2008. A selective blocker of Kv1.2 and Kv1.3  
463 potassium channels from the venom of the scorpion *Centruroides suffusus suffusus*.  
464 *Biochem.Pharmacol.* 76:1142-1154.

- 465 Delepierre, M., Prochnicka-Chalufour, A. and Possani, L.D., 1997. A novel potassium channel  
466 blocking toxin from the scorpion *Pandinus imperator*: a  $^1\text{H}$ -NMR analysis using a nano-  
467 NMR probe. *Biochemistry* 36, 2649-2658.
- 468 Delepierre, M., Prochnicka-Chalufour, A. and Possani, L.D., 1998.  $^1\text{H}$ -NMR structural analysis  
469 of novel potassium blocking toxins using a nano-NMR probe. *Toxicon* 36, 1599-1608.
- 470 Delepierre, M., Prochnicka-Chalufour, A., Boisbouvier, J. and Possani, L.D., 1999. Pi7, an  
471 orphan peptide isolated from the scorpion *Pandinus imperator*:  $^1\text{N}$ -NMR analysis using a  
472 nano-nmr probe. *Biochemistry* 38, 16756-16765
- 473 ElFessi-Magouri, R., Peigneur, S., Khamessi, O., Srairi-Abid, N., ElAyeb, M., Mile, B.G.,  
474 Tytgat, J., Kharrat, R., 2016. Kbot55, purified from *Bothus occitanus tunetanus* venom,  
475 represents the first member of a novel  $\alpha$ -KTx subfamily. *Peptides* 80, 4-8.
- 476 Garcia, M.L., Hanner, M., Kaczorowski, G.J., 1998. Scorpion toxins: tools for studying  $\text{K}^+$ -  
477 channels. *Toxicon* 36, 1641-1650.
- 478 Gómez-Lagunas, F., Olamendi-Portugal, T., Zamudio, F.Z. and Possani, L.D., 1996. Two novel  
479 toxins from the venom of the scorpion *Pandinus imperator* show that the N-terminal  
480 amino acid sequence is important for their affinities toward the Shaker B  $\text{K}^+$ -channels. *J.*  
481 *Membr. Biol.* 152, 49-56.
- 482 Gomez Lagunas, F., T. Olamendi Portugal, and L.D. Possani. 1997. Block of ShakerB  $\text{K}^+$   
483 channels by Pi1, a novel class of scorpion toxin. *FEBS Letters* 400:197-200.

- 484 Grissmer, S., A.N. Nguyen, J. Aiyar, D.C. Hanson, R.J. Mather, G.A. Gutman, M.J.  
485 Karmilowicz, D.D. Auperin, and K.G. Chandy. 1994. Pharmacological characterization  
486 of five cloned voltage-gated K<sup>+</sup> channels, types Kv1.1, 1.2, 1.3, 1.5, and 3.1, stably  
487 expressed in mammalian cell lines. *Mol.Pharmacol.* 45:1227-1234.
- 488 Guijarro, J.I., M'Barek, S., Gómez-Lagunas, F., Garnier, D., Rochat, H., Sabatier, J.M., Possani,  
489 L.D. and Delepierre, M., 2003. Solution structure of Pi4, a short four-disulfide-bridged  
490 scorpion toxin specific of potassium channels. *Protein Science* 12:1844-1854.
- 491 Islas, L.D. and Sigworth, F.J., 1999. Voltage sensitivity and gating charge in *Shaker* and *Shab*  
492 family potassium channels. *J. Gen. Physiol.* 114, 723-742.
- 493 Klaiber, K., Williams, N., Roberts, T.M., Papazian, D.M., Jan, L.Y., Miller, C., 1990. Functional  
494 expression of Shaker B K<sup>+</sup>-channels in a baculovirus-infected insect cell line. *Neuron* 5,  
495 221-226.
- 496 Kuzmenkov, A.I., Krylov, N., Chugunov, A.O., Grishin, E.V. and Vassilevski, A.A. 2016.  
497 Kalium: a database of potassium channel toxins from scorpion venom. Database, Vol  
498 2016, article ID baw056; doi: 10.1093/database/baw056.
- 499 M'Barek, S., Mosbah, A., Sandoz, G., Fajloun, Z., Olamendi-Portugal, T., Rochat, H., Sampieri,  
500 F., Guijarro, J.I., Mansuelle, P., Delepierre, M., De Waard. M., Sabatier, J.M. 2003.  
501 Synthesis and characterization of Pi4, a scorpion toxin from *Pandinus imperator* that acts  
502 on K<sup>+</sup> channels. *Eur. J. Biochem.* 270:3583-3592.
- 503 Mouhat, S., Mosbah, A., Visan, V., Wulff, H., Delepierre, M., Darbon, H., Grissmer, S., De  
504 Waard, M. and Sabatier, J.M. 2004. The 'functional' dyad of scorpion toxin Pi1 is not

- 505 itself a prerequisite for toxin binding to the voltage-gated Kv1.2 potassium channels.  
506 Biochem.J. 377:25-36.
- 507 Olamendi-Portugal, T., Gómez-Lagunas, F., Gurrola, G.B. and Possani, L.D., 1996. A novel  
508 structural class of K<sup>+</sup> channel blocking toxin from the scorpion *Pandinus imperator*,  
509 Biochem J. (London) 315, 977-981.
- 510 Olamendi-Portugal, T., Gomez-Lagunas, F., Gurrola, G.B. and Possani, L.D., 1998. Two similar  
511 peptides from the venom of the scorpion *Pandinus imperator*, one highly effective  
512 blocker and the other inactive on K<sup>+</sup> channels. Toxicon 36, 759-770.
- 513 Olamendi-Portugal, T., Bartok, A., Zamudio-Zuñiga, F., Balajthy, A., Becerril, B., Panyi, G.  
514 Possani, L.D., 2016. Isolation, chemical and functional characterization of several new  
515 K<sup>+</sup>-channel blocking peptides from the venom of the scorpion *Centruroides tecomanus*.  
516 Toxicon 115, 1-12.
- 517 Peter, M., P. Hajdu, Z. Varga, S. Damjanovich, L.D. Possani, G. Panyi, and R. Gaspar. 2000.  
518 Blockage of human T lymphocyte Kv1.3 channels by Pi1, a novel class of scorpion toxin.  
519 Biochem. Biophys. Res. Commun. 278:34-37.
- 520 Peter, M., Jr., Z. Varga, P. Hajdu, R. Gaspar, Jr., S. Damjanovich, E. Horjales, L.D. Possani, and  
521 G. Panyi. 2001. Effects of toxins Pi2 and Pi3 on human T lymphocyte Kv1.3 channels:  
522 the role of Glu7 and Lys24. J Membr.Biol 179:13-25.
- 523 Possani, L.D., Becerril, B., Delepierre, M. and Tytgat, J., 1999. Scorpion toxins specific for Na<sup>+</sup>-  
524 channels. Eur. J. Biochem. 264, 287-300.

- 525 Rodríguez de la Vega, R. and Possani, L.D., 2004. Minireview: Current views on scorpion toxins  
526 specific for K<sup>+</sup>-channels. *Toxicon* 43, 865-875.
- 527 Rogowski, R.S., Collins, J.H., O'Neil, T.J., Gustafson, T.A., Werkman, T.R., Rogwaski, M.A.  
528 Tenenholz, T.C. Weber, D.J. and Blaustein, M.P. 1996. Three new toxins from the  
529 scorpion *Pandinus imperator* selectively block certain voltage-gated K- channels. *Mol.*  
530 *Pharmacol.* 50:1167-1177.
- 531 Tytgat, J., Chandy, K.G., Garcia, L.M., Gutman, G.A., Martin-Eauclaire, M.F., van del Walt, J.J.  
532 and Possani, L.D.. 1999. A unified nomenclature for short chain peptides isolated from  
533 scorpion venoms: alpha-KTx molecular subfamilies. *Trends in Pharmacol. Sciences* 20,  
534 445-447.
- 535 Zamudio, F.Z., Gurrola, G.B., Arévalo, C., Sreekumar, R., Walker, J.W., Valdivia, H.H. and  
536 Possani, L.D., 1997a. Primary structure and synthesis of imperatoxin A (IpTx<sub>a</sub>), a  
537 peptide activator of Ca<sup>2+</sup> release channels/ryanodine receptors. *FEBS Lett.* 405, 385-389.
- 538 Zamudio, F.Z., Conde, R., Arévalo, C., Becerril, B., Martin, B.M., Valdivia, H.H. and Possani,  
539 L.D., 1997b. The mechanism of inhibition of ryanodine receptor channels by imperatoxin  
540 I, a heterodimeric protein from the scorpion *Pandinus imperator*. *J. Biol.Chem.* 272,  
541 11886-11894.

542

543

**544 FIGURE LEGENDS**

545

**546 Figure 1: Purification and amino acid sequence of Pi5 and Pi6**

547 A. Fraction III from Sephadex G-50 column (0.5 mg) was separated by HPLC using an  
 548 analytical C18 reverse-phase column (4.6 x 250 mm), with a linear gradient from solution A  
 549 (0.12% trifluoacetic acid –TFA- in water) to 40% solution B (0.10% TFA in acetonitrile). Sub-  
 550 fraction 5 (labeled with asterisk) was homogeneous Pi5, which was digested with chymotrypsin  
 551 and separated again in the same conditions, as indicated in the inset figure labeled Pi5. The  
 552 asterisk indicates the peptide whose sequence allowed completion of the amino acid sequence  
 553 shown in letter B, from position 26 to 33 (under labeled with .Ch.). Similarly, the sub-fraction 6  
 554 (labeled with asterisk) was the homogeneous peptide Pi6, which was digested with Protease V8  
 555 from *Staphylococcus aureus*, and separated in the same conditions, as indicated in the insert  
 556 labeled Pi6. The labeled peptide with asterisk was sequenced and permitted completion of the  
 557 sequence from amino acids in position 21 to 28 (underlined .V8.). Letters B and C show the full  
 558 amino acid sequence for both peptides, where “Direct” means amino acid sequence obtained  
 559 with a reduced and alkylated sample of each peptide.

560

561 **Figure 2: Effect of Pi5 on *Drosophila* K<sup>+</sup> channels**

562 (A) K<sup>+</sup> currents through *dShaker B* channels. K<sup>+</sup>-currents were elicited every 15-sec by 30-ms  
 563 pulses from -20 to +60 mV applied in 10 mV increments from a holding potential of -80 mV,  
 564 before (left panel, labeled Control), during (middle panel, labeled Pi5) and after (labeled  
 565 Recovery) the addition of 1.5 μM Pi5 to the external solution. (B) Current-Voltage relationship  
 566 of the traces in A: closed circles: control I<sub>K</sub>, open symbols: I<sub>K</sub> with 1.5 μM Pi5 in the external  
 567 solution, closed triangles: I<sub>K</sub> after washing the cell with the control solution. The inset shows  
 568 that the block (1.5 μM Pi5) is not voltage dependent. (C) Fractional block vs. [Pi5], the fractional  
 569 block (F.b) was calculated as  $F.b = 1 - (I/I_0)$ , where I<sub>0</sub> and I are the peak current in the control and  
 570 in the presence of Pi5, respectively. The line is the least squares fit of the points with the  
 571 Michaelis-Menten equation, with K<sub>d</sub>= 540 nM. The inset shows the expected linear double-  
 572 reciprocal plot of the points (r=0.995). (D) K<sup>+</sup> currents through *dShab* channels. The figure  
 573 shows two superimposed currents evoked by a 30mV/30ms pulse applied from -80 mV, before  
 574 and during addition of 1.5 μM Pi5, as indicated. (E) Current-voltage relationship before and in  
 575 the presence of 1.5 μM Pi5 from traces as in D. There was no blockage.

576

**577 Figure 3: Block of Kv1.2 and Kv1.3 channels by Pi5**

578 A) Whole-cell potassium currents through hKv1.2 channels were evoked from a transiently  
579 transfected CHO cells in response to depolarizing pulses to +50 mV from a holding potential of -  
580 100 mV every 15s. The current traces were recorded in the absence of the toxins (control,  
581 indicated by arrow), after equilibration of the block in the presence of Pi5 (indicated by arrow) in  
582 100 nM concentration. Charybdotoxin (ChTx, arrow, 14 nM) was used as a positive control. B)  
583 Development of and recovery from block of Kv1.2 by Pi5. Peak currents were determined during  
584 repeated depolarizations to +50 mV, arrows indicate the start of the bath perfusion with 100 nM  
585 Pi5 or with the toxin-free bath solution (labeled “wash”). C) Double-reciprocal plot of the dose-  
586 response of Pi5 on hKv1.2. See methods for details. The linear regression ( $1/B=(Kd*1/C)+1$ )  
587 resulted in a Kd of 92 nM ( $R^2=0.99$ ). D) Whole-cell potassium currents through hKv1.3 channels  
588 were evoked from in activated human peripheral lymphocytes in response to depolarizing pulses  
589 to +50 mV from a holding potential of -100 mV every 15s. The current traces were recorded in  
590 the absence of the toxins (control, indicated by arrow), after equilibration of the block in the  
591 presence of Pi5 in 100 nM concentration (arrow). Tetraethylammonium (TEA, arrow, 10 mM)  
592 was used as a positive control. D) Development of and recovery from block of Kv1.3 by Pi5.  
593 Peak currents were determined during repeated depolarizations to +50 mV, arrows indicate the  
594 start of the bath perfusion with 10 nM Pi5 or 100 nM Pi5 or the toxin-free bath solution (arrow  
595 labeled wash). E) Double-reciprocal plot of the dose-response of Pi5 on hKv1.3. See methods  
596 for details. The linear regression ( $1/B=(Kd*1/C)+1$ ) resulted in a Kd of 77 nM ( $R^2=0.99$ ).

597

**598 Figure 4: Block of Kv1.2 and Kv1.3 channels by Pi6**

599 A) Whole-cell potassium currents through hKv1.2 channels were evoked from a transiently  
600 transfected CHO cells in response to depolarizing pulses to +50 mV from a holding potential of -  
601 100 mV every 15s. The current traces were recorded in the absence of the toxins (control,  
602 indicated by arrow), after equilibration of the block in the presence of Pi6 (indicated by arrow) in  
603 100 nM concentration. Charybdotoxin (ChTx, arrow, 14 nM) was used as a positive control. B)  
604 Development of and recovery from block of Kv1.2 by Pi6. Peak currents were determined during  
605 repeated depolarizations to +50 mV, arrows indicate the start of the bath perfusion with 100 nM  
606 Pi6 or with the toxin-free bath solution (labeled “wash”). C) Whole-cell potassium currents

607 through hKv1.3 channels were evoked from in activated human peripheral lymphocytes in  
 608 response to depolarizing pulses to +50 mV from a holding potential of -100 mV every 15s. The  
 609 current traces were recorded in the absence of the toxins (control, indicated by arrow), after  
 610 equilibration of the block in the presence of Pi6 in 100 nM concentration (arrow).  
 611 Tetraethylammonium (TEA, arrow, 10 mM) was used as a positive control. D) Development of  
 612 and recovery from block of Kv1.3 by Pi6. Peak currents were determined during repeated  
 613 depolarizations to +50 mV, arrows indicate the start of the bath perfusion with 100 nM Pi6 or the  
 614 toxin-free bath solution (arrow labeled wash).

615

#### 616 **Figure 5: Selectivity profile of Pi5 and Pi6**

617 A) Bars indicate the remaining current fractions at equilibrium block of the indicated channels by  
 618 100 nM Pi5 (empty bars) or 100 nM Pi6 (hatched bars). For the expression systems, solutions  
 619 and voltage protocols see Materials and Methods and Figs 2-4 and supplementary Fig. 2. Error  
 620 bars indicate SEM (n=3-6).

621

#### 622 **Figure 6: Comparative sequences of *Pandinus imperator* toxins**

623 Amino acid sequences of the K<sup>+</sup>-channel peptides isolated from *Pandinus imperator* and  
 624 percentage of identity (Iden.) compared to Pi1. Cons.1 and Cons.2 stand for consensus on the  
 625 relative positions of the cysteine residues in Pi1-Pi4, Pi7 and Pi5, Pi6, respectively. Amino acids  
 626 in identical positions are highlighted in gray. References (ref) in this figure correspond to: (1)  
 627 (Mouhat et al., 2004), (2) (Peter et al., 2000), (3) (Gomez Lagunas et al., 1997), (4) (Rogowski et  
 628 al., 1996), (5) (Peter et al., 2001), (6) (Gomez-Lagunas et al., 1996), (7) (M'Barek et al., 2003)  
 629 and (8) (Olamendi-Portugal et al., 1998).

630

#### 631 **Figure 7: Unrooted phylogenetic tree of $\alpha$ -KTx**

632 A multiple sequence alignment of 30 sequences were retrieved from public databases, literature  
 633 or unpublished results from our laboratory. The evolutionary history was inferred using the  
 634 Neighbor-Joining method. The tree is drawn to scale, with branch lengths in the same units as  
 635 those of the evolutionary distances used to infer the phylogenetic tree. The evolutionary



636 distances were computed using the Poisson correction method and are in the units of the number  
637 of amino acid substitutions per site. Evolutionary analyses were conducted in MEGA7.

638

639 **Figure 8: Amino acid sequence of the family  $\kappa$ -KTx 2**

640 Pi6 is the number 9 of this subfamily.

641

642 **Legend for Supplementary Figures**

643

644 **Supplementary Figure 1: Pi6 effect on Shaker channels**

645 Pi6 does not inhibit *Shaker* channels. *Shaker*  $I_K$  evoked by delivering 30-ms activation pulses  
646 from -40 to +50 mV, in 10 mV increments, before (left panel), and after addition of 100 nM Pi6  
647 to the extracellular solution (right panel).  $I_K$  was not significantly inhibited by Pi6. HP= -80 mV.  
648 Time between pulses was 20-sec to allow full recovery from inactivation.

649

650 **Supplementary Figure 2: Lack of inhibition of hKv1.1 and hKv1.4 by Pi5 and Pi6**

651 A, C) Whole-cell potassium currents through hKv1.1 (A) or hKv1.4 channels (C) were evoked  
652 from a transiently transfected CHO cells in response to depolarizing pulses to +50 mV from a  
653 holding potential of -100 mV every 15s. The current traces were recorded in the absence of the  
654 toxins (control, indicated by arrow), after at least 10 episodes in of Pi5 or Pi6 (indicated by  
655 arrows) in 100 nM concentration. Tetraethylammonium (TEA, arrow, 0.3 mM) was used as a  
656 positive control in A. Positive control for hKv1.4 was obtained by perfusing the recording  
657 chamber with a bath solution containing 150 mM  $K^+$  (not shown). B,D) Peak hKv1.1 (B) and  
658 hKv1.4 currents (D) in 100 nM Pi5 or Pi6. Peak currents were determined during repeated  
659 depolarizations to +50 mV, arrows indicate the start of the bath perfusion with 100 nM Pi5 or  
660 100 nM Pi6.

661

662 **Supplementary Figure 3: Amino acid sequence of  $\alpha$ -KTx toxins**

663 Only the number 1 toxin of each subfamily was selected. The number  $\alpha$ -KTx 25 is empty.

664

665

666

667

668

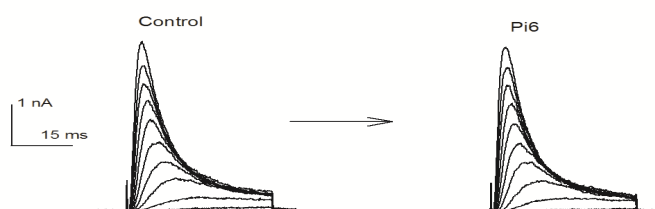
669

670

671

672

673



674 **Supplementary Figure 1: Pi6 effect on Shaker channels**

675 Pi6 does not inhibit *Shaker* channels. *Shaker*  $I_K$  evoked by delivering 30-ms activation pulses

676 from -40 to +50 mV, in 10 mV increments, before (left panel), and after addition of 100 nM Pi6

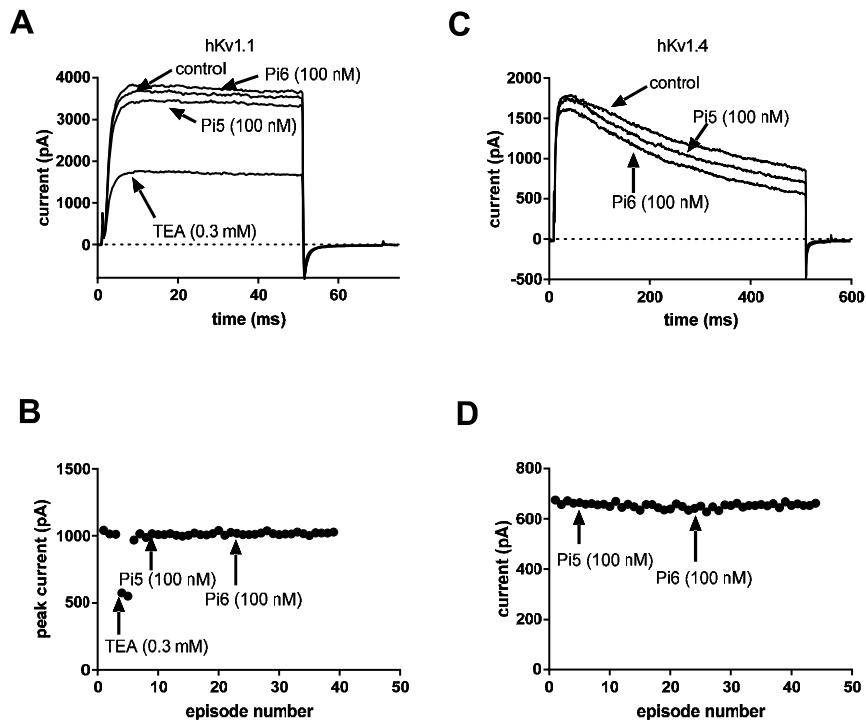
677 to the extracellular solution (right panel).  $I_K$  was not significantly inhibited by Pi6. HP= -80 mV.

678 Time between pulses was 20-sec to allow full recovery from inactivation.

679

680

681



682  
 683  
 684 **Supplementary Figure 2:** Pi6 does not inhibit Shaker channels. Shaker IK evoked by  
 685 delivering 30-ms activation pulses from -40 to +50 mV, in 10 mV increments, before (left panel),  
 686 and after addition of 100 nM Pi6 to the extracellular solution (right panel). IK was not  
 687 significantly inhibited by Pi6. HP= -80 mV. Time between pulses was 20-sec to allow full  
 688 recovery from inactivation.

689

690

### 691 **Supplementary Figure 3: Amino acid sequence of $\alpha$ -KTx toxins**

692 • -KTx-1.1 QFTNVSC TTSKECWSVCQRLHNTSRGKCMNKKRCYS  
 693 • -KTx-2.1 TIINVKCTSPKQCSKPCKELYGSSAGAKCMNGKCKCYNN  
 694 • -KTx-3.1 GVEINVKCSGSPQCLKPKCDAGMRFGKCMNRKCHCTPK  
 695 • -KTx-4.1 VFINAKCRGSPECLPKCKEAI GKAAGKCMNGKCKCYP  
 696 • -KTx-5.1 AFCNLRMCQLSCLSLGLLGKCI GDKCECVKH  
 697 • -KTx-6.1 LVKCRGTSDCGRPCQQQTGCPNSKCI INRMCKCYGC  
 698 • -KTx-7.1 TISCTNPKQCYPHCKKETGYPNAKCMNRKCKCFGR  
 699 • -KTx-8.1 VSCEDCPEHCSTQKAQAKCDNDKCVCEPI  
 700 • -KTx-9.1 VGCEECPMHCKGKNAKPTCDDGVCNCNV

701 •-KTx-10.1 AVCVYRTCDKDKRRGYRSGKGINNACKCYPY  
 702 •-KTx-11.1 DEEPKESCSDEMCIYCKGEEYSTGVCDGPQKCKCSD  
 703 •-KTx-12.1 WCSTCLDLACGASRECYDPCFKAFGRAHGKCMNNKRCRYT  
 704 •-KTx-13.1 ACGSCRKCKGSGKCIINGRCKCY  
 705 •-KTx-14.1 TPFAlKCATDADCSRKCPGNPSCRNGFCACT  
 706 •-KTx-15.1 QNETNKKCQGGSCASVCRRVIGVAAGKCIINGRCVCYP  
 707 •-KTx-16.1 DLIDVKCISSQECWIACKKVTGRFEGKCQNRQCRCY  
 708 •-KTx-17.1 QTQCQSVRDCQQYCLTPDRCSYGTICYCKTT  
 709 •-KTx-18.1 TGPQTTQAAMCEAGCKGLGKSMESCQGDTCCKCA  
 710 •-KTx-19.1 AACYSDDCRVKCVAMGFSSGKCIINSKCKCYK  
 711 •-KTx-20.1 GCTPEYCSMWCKVKVSQNYCVKNCKCPGR  
 712 •-KTx-21.1 GKFGKCKPNICAKTCQTEKGGMGYCNKTECVCSSEW  
 713 •-KTx-22.1 EVDGRTATFCTQSICEESCKRQNKNGRCVIEAEGSLIYHLCKCY  
 714 •-KTx-23.1 AAAISCVGSPECPPKCRAQGCKNGKCMNRKCKCYC  
 715 •-KTx-24.1 VAKCSTSECGHACQQAGCRNSGCRYGSCICVGC  
 716 •-KTx-25.1 Empty  
 717 •-KTx-26.1 NFKVEGACSKPCRKYCIDKGARNGKCIINGRCHCY  
 718 •-KTx-27.1 QIDINVSCRYGSDCAEPCKRLKCLLPSKCIINGKCTCYPsIKIKNCKVQTY  
 719 •-KTx-28.1 ACVTHECTLLCYDTIGTCVDGKCKCM  
 720 •-KTx-29.1 EGDCEPISAEIKCVEKCKEKEVECEPGVCKCSG  
 721 •-KTx-30.1 EDKLGKTKTDDCAKYCSQFTDVHPACLGGYCECLRWEGLISS  
 722 •-KTx-31.1 AGSMDSCSETGVCMKACSERIRQVENDNKCPAGECICTT

723  
724

725 Only the first the number 1 toxin of each subfamily was selected. The number  $\alpha$ -KTx 25 is empty

726  
727

728

**Highlights**

1. Two short length peptides: Pi5 and Pi6 were purified and characterized from *Pandinus imperator* scorpion venom.
2. Pi5 has 33 amino acids and constitutes a new subfamily of  $\alpha$ -KTx, (systematic number  $\alpha$ -KTx 24.1).
3. Pi6 contains 28 amino acids, two disulfide bonds, and is a new member of the  $\kappa$ -KTx (systematic number  $\kappa$ -KTx2.9).
4. Pi5 inhibited *Shaker B*, hKv1, Kv1.2 and hKv1.3 channels at nanomolar concentrations.
5. Pi6 is a non-selective blocker of hKv1.2 and hKv1.3 channels.